American Journal of Physical Chemistry
2014; 3(2): 19-25
Published online May 20, 2014 (http://www.sciencepublishinggroup.com/j/ajpc)
doi: 10.11648/j.ajpc.20140302.13

Theoretical and experimental investigations on molecular structure, IR, NMR spectra and HOMO-LUMO analysis of 4-methoxy-*N*-(3-phenylallylidene) aniline

Kürşat Efil[1, 2, *], Yunus Bekdemir[2]

[1]Ondokuz Mayis University, Faculty of Arts and Sciences, Department of Chemistry, 55139- Samsun, Turkey
[2]Canik Başarı University, Faculty of Arts and Sciences, Department of Molecular Biology and Genetics, 55080-Samsun, Turkey

Email address:
kursatefil@gmail.com (K. Efil), bekdemir@basari.edu.tr (Y. Bekdemir)

To cite this article:
Kürşat Efil, Yunus Bekdemir. Theoretical and Experimental Investigations on Molecular Structure, IR, NMR Spectra and HOMO-LUMO Analysis of 4-Methoxy-*N*-(3-Phenylallylidene) Aniline. *American Journal of Physical Chemistry.* Vol. 3, No. 2, 2014, pp. 19-25.
doi: 10.11648/j.ajpc.20140302.13

Abstract: In this study, 4-Methoxy-*N*-(3-phenylallylidene) aniline has been synthesized and characterized by FTIR and NMR spectroscopic techniques. The optimized geometrical structure, vibrational frequencies and NMR shifts of title molecule were obtained by using ab initio HF and density functional method (B3LYP) with 6-31G* basis set. The experimental and calculated geometrical parameters were compared with each other. The calculated infrared (IR) and NMR data were compared with experimental values using HF and B3LYP/6-31G* level of theory. It was found to be a good correlation between experimental and calculated data. In addition, HOMO and LUMO analysis of title molecule were calculated using corresponding methods with 6-31G* basis set. The calculated HOMO-LUMO energies were used to calculate some properties of title molecule.

Keywords: 4-Methoxy-*N*-(3-Phenylallylidene) Aniline, B3LYP, Hartree–Fock, IR and NMR Spectra, HOMO-LUMO

1. Introduction

The compounds having the C=N group, are known as Schiff bases (also imines or azomethines), are generally synthesized by condensation of primary amines with active carbonyl compounds [1,2], The reaction is acid-catalyzed and is usually performed by refluxing the carbonyl compound and amine [3]. Schiff bases attracted much attention as they show broad spectrum of biological activities, such as antitumor [4], anticancer [5], antifungal [6], antimicrobial [7] and antiviral agents [8], furthermore they have effect as corrosion inhibitors [9,10].

We know that the quantum chemical calculations for 4-Methoxy-N-(3-phenylallylidene) aniline (MPA) have not been reported so far. In this study, optimized geometrical parameters, IR vibrational frequencies and NMR chemical shifts of MPA were computed by HF and density functional method (B3LYP) with 6-31G* basis set. The results obtained were compared with literature and our experimental ones. In addition, HOMO and LUMO analysis of title molecule were calculated using corresponding methods with 6-31G* basis set. The calculated HOMO-LUMO energies were used to calculate some properties such as ionization potential, electron affinity, electrophilicity index, chemical potential, electronegativity, chemical hardness, and softness of MPA.

2. Experimental Details

2.1. Synthesis

4-Methoxyaniline (0.123g, 1 mmol), *trans*-cinnamaldehyde (0.132g, 1 mmol) and two drops of β-ethoxyethanol as a wetting reagent were mixed in a beaker. Then the beaker was placed in the microwave oven and was exposed to microwave irradiation (360 W). The product obtained by reaction was washed with cold ethanol. Then, it was recrystallized in ethanol. The MPA molecule was synthesized in our previous study[11].

The infrared absorption spectrum of MPA was recorded using a Bruker Vertex 80/80v spectrophotometer at room temperature. ^{1}H-NMR and ^{13}C-NMR spectra were recorded in $CDCl_3$ at 200 MHz in a Bruker AC spectrometer using TMS as the internal standard.

3. Quantum Chemical Calculation

The molecular structure of MPA was optimized using HF and B3LYP method at 6-31G* level of the theory with the Gaussian 03 package program [12]. IR vibration frequencies and NMR chemical shifts were computed from the Gaussian output files. The vibrational frequency assignments were made using Gauss-View program [13]. The calculated frequencies were scaled by 0.8929 for HF/6-31G* and 0.9613 for B3LYP/6-31G*, respectively [14]. The NMR isotropic shielding constants were calculated using the standard GIAO (Gauge-Independent Atomic orbital) approach [14,15] of the Gaussian 03 package. The GIAO NMR calculations were carried out in both solvent (chloroform) and gas phase using the corresponding methods. In addition, HOMO and LUMO energies of MPA were calculated by HF and B3LYP methods with corresponding basis set.

4. Result and Discussion

4.1. Molecular Structure

The optimized structure and atomic numbering of MPA molecule are illustrated in Fig. 1. The energy of MPA molecule is calculated as -743.903997 a.u for HF/6-31G* and -748.678925 a.u for B3LYP/6-31G*, respectively. The experimental bond lengths, bond angles and dihedral angles and the optimized ones obtained by HF and B3LYP methods combining with 6-31G* basis set for MPA molecule are listed in Table 1. As seen from the Table 1, the experimental bond length of C7-C8 with HF and of O1-C16 with B3LYP method is equal. The coefficients of determination (R^2) between experimental and theoretical bond lengths are 0.954 for HF and 0.944 for B3LYP method, respectively. For the bond angles, the R^2 values are 0.906 for HF and 0.944 for B3LYP method, respectively. For the dihedral angles, C10-N1-C9-C8 dihedral angle is -179.82° for X-ray, 178.75° for HF and 177.56° for B3LYP method, therefore the molecule has trans configuration by C9-N1(>C=N-) bond. The dihedral angle of C9-C8-C7-C6 is 176.14° for X-ray, 179.91° for HF and 179.83° for B3LYP method, therefore the molecule has trans configuration by C8-C7 (>C=C<) bond.

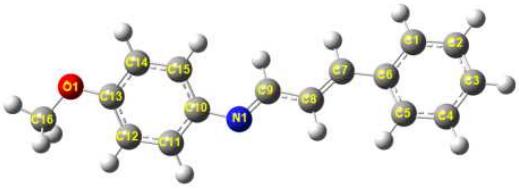

Figure 1. *The optimized structure of 4-Methoxy-N-(3-phenylallylidene) aniline at B3LYP/6-31G* level.*

Table 1. *The experimental (X-ray) and calculated bond lengths (Å), bond angles (°), dihedral angles (°) for HF and B3LYP/6-31G* methods of MPA.*

Bond Length (Å)	X-ray[17]	HF	B3LYP	Bond Angle (°)	X-ray[17]	HF	B3LYP
C1-C2	1.379	1.385	1.393	C13-C14-C15	120.35	120.49	120.44
C1-C6	1.397	1.392	1.408	C14-C15-C10	120.78	120.84	120.87
C2-C3	1.379	1.383	1.396	C15-C10-C11	118.00	118.10	117.92
C3-C4	1.380	1.388	1.399	C15-C10-N1	124.29	124.07	124.80
C4-C5	1.378	1.381	1.391	C13-O1-C16	117.53	119.63	118.21
C5-C6	1.394	1.396	1.410	O1-C13-C12	124.90	124.76	124.83
C6-C7	1.465	1.475	1.462	O1-C13-C14	115.29	115.96	115.69
C7-C8	1.329	1.329	1.352		Dihedral angle (°)		
C8-C9	1.442	1.463	1.447	O1-C13-C14-C15	−178.76	-179.76	-179.70
C9-N1	1.275	1.258	1.288	C12-C13-C14-C15	0.2	0.9	1.1
N1-C10	1.413	1.408	1.403	C13-C14-C15-C10	0.2	0.1	-0.2
C10-C11	1.386	1.385	1.402	O1-C13-C12-C11	177.96	-179.52	-179.30
C11-C12	1.390	1.387	1.394	C14-C13-C12-C11	−0.9	-0.2	-0.2
C12-C13	1.384	1.386	1.401	C10-C11-C12-C13	1.2	-1.44	-1.7
C13-C14	1.390	1.391	1.404	C12-C13-O1-C16	0.1	0.6	0.1
C14-C15	1.380	1.378	1.386	C14-C13-O1-C16	179.01	-178.71	-179.07
C15-C10	1.398	1.396	1.411	C6-C5-C4-C3	0.6	0.2	0.0
C13-O1	1.375	1.350	1.365	C2-C3-C4-C5	−1.2	0.2	0.0
O1-C16	1.418	1.398	1.418	C10-N1-C9-C8	−179.82	178.75	177.56
	Bond angle (°)			C7-C8-C9-N1	−170.20	179.82	179.87
C1-C2-C3	119.89	120.00	120.02	C4-C3-C2-C1	0.5	-0.1	0.0
C1-C6-C7	119.72	118.75	118.83	C6-C1-C2-C3	0.8	-0.2	0.0
C1-C6-C5	117.99	118.23	117.95	C9-C8-C7-C6	176.14	179.91	179.83
C2-C1-C6	121.14	121.12	121.24	C4-C5-C6-C1	0.7	-0.5	0.0
C2-C3-C4	119.80	119.54	119.54	C4-C5-C6-C7	−177.93	179.69	-180.00
C3-C4-C5	120.52	120.39	120.44	C2-C1-C6-C5	−1.4	0.5	0.0
C4-C5-C6	120.64	120.71	120.81	C2-C1-C6-C7	177.27	-179.63	-180.00
C5-C6-C7	122.28	123.02	123.22	C8-C7-C6-C5	23.2	-8.6	-0.4

Bond Length (Å)	X-ray[17]	HF	B3LYP	Bond Angle (°)	X-ray[17]	HF	B3LYP
C6-C7-C8	125.90	127.57	127.80	C8-C7-C6-C1	−155.4	171.54	179.66
C7-C8-C9	123.60	122.04	122.44	C12-C11-C10-C15	−0.8	2.4	2.5
C8-C9-N1	122.08	121.19	121.24	C12-C11-C10-N1	−178.40	-179.82	-179.60
C9-N1-C10	119.80	120.49	120.60	C14-C15-C10-C11	0.1	1.7	-1.6
N1-C10-C11	117.67	117.80	117.24	C14-C15-C10-N1	177.50	-179.34	-179.28
C10-C11-C12	121.79	121.52	121.64	C9-N1-C10-C11	−150.54	145.22	152.80
C11-C12-C13	119.29	119.75	119.61	C9-N1-C10-C15	32.0	-37.1	-29.5
C12-C13-C14	119.79	119.27	119.47				

The potential energy surfaces (PES) scan with the semi-empirical quantum chemistry method (AM1) level of theoretical approximations was performed for MPA molecule by varying the dihedral angle D1(C11-C10-N1-C9) and D2(N1-C9-C8-C7) in steps of 10º from -180 to 180º. The resultant minimum energy curve belong to selected dihedral angles of MPA molecule is shown in Fig. 2. According to X-ray crystallographic study, dihedral angle, D1(C11-C10-N1-C9) and D2(N1-C9-C8-C7) were determined as -150.54º and -170.20º, respectively[17]. In this study, dihedral angle D1 of MPA molecule was determined as 145.22º for HF and as 152.80º for B3LYP method, and dihedral angle D2 was determined as 179.82º for HF and as 179.87º for B3LYP method. The dihedral angle D1 has one energy maxima as 0º and D2 have two energy maxima as -100º and 90º. The maximum energies were obtained at 60.4 kcal mol^{-1} for dihedral angle D1 and 55.3 and 55.2 kcal mol^{-1} for dihedral angle D2, respectively. Four local minima at -150º, -50º, 50º and 150º for D1 and three local minima at -180º, -20º and 180º for D2 were observed (Fig. 2). The energy values of corresponding local minima were found as 53.6, 55.6, 55.5 and 53.2 kcal mol^{-1} for D1 and as 53.2, 53.4, 53.2 kcal mol^{-1} for D2, respectively. These local minima are the most stable conformers for MPA molecule. The energy difference between the most favorable and unfavorable conformers, arises from the rotational potential barrier with respect to the selected torsion angle, was calculated to be 7.2 and 2.1 kcal mol^{-1} for the torsional angle D1 and D2 of MPA molecule.

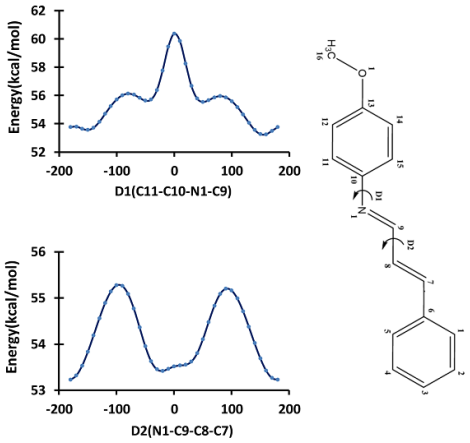

Figure 2. *The rotational bond names, atomic numbering scheme and potential energy surface scan for dihedral angle D1(C11-C10-N1-C9) and D2(N1-C9-C8-C7) of MPA.*

4.2. Vibrational Analysis

4.2.1. C–H Vibrations

The characteristic C–H stretching vibrations of the phenyl ring is observed at 3000-3100 cm^{-1} [18]. Two bands observed at 3014 and 3037 cm^{-1} in experimental IR spectra are the results of the coupling of the C-H stretching vibration of the phenyl ring and C-H stretching of H-C(7)=C(8)-H. The calculated values are at 3012 and 3020 cm^{-1} for HF, 3071 and 3084 cm^{-1} for B3LYP, respectively. Aliphatic C-H stretching vibrations of MPA molecule are observed at 2836, 2884(NC-H), 2939 and 2961 cm^{-1}, while the calculated values are 2863, 2898, 2917 and 2969 cm^{-1} for HF, 2908, 2965, 3021 and 3035 cm^{-1} for B3LYP, respectively. The C–H bending bands appear in the regions 1275–1000 cm^{-1} (in-plane bending) and 900–690 cm^{-1} (out-of plane bending) [18]. The C-H bending vibrations of aromatic and aliphatic groups are observed at 1448, 1464 and 1500 cm^{-1}. The calculated ones are at 1444, 1493, 1512 cm^{-1} for HF, 1440, 1486, 1496 cm^{-1} for B3LYP with 6-31G*, respectively.

4.2.2. C=N and C=C Vibrations

The characteristic C=N stretching vibration bands of imines is observed at 1690-1640 cm^{-1} [19]. In a literature study, the vibration bands of C=N was observed at 1659-1619 cm^{-1}[20]. In our study, the stretching vibration of C=N was shifted to 1622 cm^{-1} due to conjugation of C=N bond with the aromatic ring. The calculated value of C=N stretching frequency is 1699 cm^{-1} for HF and 1616 cm^{-1} for B3LYP, respectively. Unconjugated C=C vibration bands have stretching frequency in the region 1620-1680 cm^{-1} for alkenes. Conjugation of the C=C bond with a double bonds or an aromatic rings decrease the frequency of the bond [21]. The C=C stretching vibration neighboring to the C=N bond and aromatic ring was observed at 1622 cm^{-1}. The calculated value was at 1699 for HF and 1630 cm^{-1} for B3LYP. The aromatic C=C stretching vibrations were observed at 1604 and 1576 cm^{-1}. They were calculated as 1625 and 1583 cm^{-1} for HF and 1598 and 1557 cm^{-1} for B3LYP method.

4.2.3. C-O Vibrations

The spectra of aryl alkyl ethers display an asymmetrical C-O-C stretching band at 1275-1200 $cm^{-1}$and symmetrical stretching near at 1075-1020 cm^{-1}[22]. The asymmetrical and symmetrical stretching band of C-O bond was observed at 1239 and 1028 cm^{-1}, respectively. The asymmetrical

stretching band was calculated as 1277 for HF and 1252 cm^{-1} for B3LYP, and the symmetrical stretching band as 1059 for HF and 1038 cm^{-1} for B3LYP with 6-31G*, respectively.

The calculated vibrational frequencies were compared with their experimental data by R^2 which were 0.9992 (y = 0,9826x + 52,932) for HF, 0.9995 (y = 1,0419x - 57,753) for B3LYP and 6-31G* basis set, respectively. It was seen that the results of B3LYP/6-31G* method gave better resemblance to the experimental measurement in the infrared analysis of MPA molecule. The experimental and calculated vibration frequencies of MPA molecule are given in Table 2. Additionally, the comparative study of infrared spectra of MPA molecule were shown in Fig. 3.

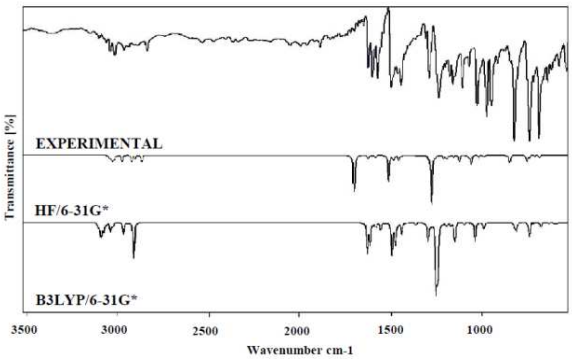

Figure 3. *The experimental and theoretical IR spectra of the MPA.*

Table 2. *Comparison of the observed and calculated some vibrational frequencies of the MPA molecule.*

Assignments	Experimental FT-IR (cm^{-1})	Calculated frequencies (cm^{-1})/6-31G*			
		HF		B3LYP	
		Unscaled	Scaled	Unscaled	Scaled
ν_sC-H	—	3406	3041	3228	3103
ν_sC-H	—	3398	3034	3214	3090
ν_{as} C-H	3037	3382	3020	3208	3084
ν_{as} C-H	3014	3373	3012	3195	3071
ν_{as} C-H	—	3354	2995	3179	3056
ν_{as}C-H, al	2961	3325	2969	3157	3035
ν_{as}C-H, al	2939	3267	2917	3143	3021
ν NC-H	2884	3246	2898	3084	2965
ν_s C-H, al	2836	3206	2863	3025	2908
ν C=C, al	1622	1903	1699	1696	1630
ν C=N	1622	1861	1662	1681	1616
ν C=C	1604	1820	1625	1662	1598
ν C=C	1576	1773	1583	1620	1557
γ C-H	1500	1693	1512	1556	1496
γ C-H	1464	1672	1493	1546	1486
α C-H	—	1661	1483	1534	1475
ω C-H	—	1631	1456	1500	1442
γ C-H	1448	1617	1444	1498	1440
ν C-O	1239	1430	1277	1302	1252
α C-H + ν C-N	—	1354	1209	1252	1204
α C-H + ν C-N	—	1340	1196	1243	1195
α C-H	—	1292	1154	1219	1172
γ C-H	—	1259	1124	1143	1099
α C-H	—	1201	1072	1113	1070
ν C-O	1028	1186	1059	1080	1038
ω C-H	—	1138	1016	1031	991
δ C-H	—	1105	987	851	818
ω C-H	—	952	850	843	810
ω C-H	—	845	754	770	740
δ C-H	—	798	712	729	700
δ C-H	—	767	685	703	676
R^2		0.9992		0.9995	

ν, stretching; γ, rocking; α, scissoring; δ, twisting; ω, wagging

4.3. ^{1}H and ^{13}C-NMR Spectra

The ^{1}H and ^{13}C NMR chemical shifts of MPA molecule have been carried out using the HF and B3LYP method with 6–31G* basis set for the optimized geometry and the results were given in Table 3. The calculations of ^{1}H and ^{13}C-NMR were carried out in both gas phase and solvent chloroform (cfm).

The average values were presented for hydrogen atoms of $-CH_3$ (H16), because they were observed as multiple signals in the calculated NMR spectra with the corresponding method and basis set. Aromatic ring protons have chemical shift in the region 6.5-8.0 ppm in ^{1}H NMR spectra [23]. In experimental ^{1}H NMR spectra, we observed the aromatic ring protons between 7.00 and 7.61 ppm. They were calculated in the region 6.76-8.16 for HF/6–31G* (gas), 6.97-8.28 ppm for HF/6–31G* (cfm) and 6.43-7.70 for B3LYP/6–31G* (gas), 6.62-7.80 ppm for B3LYP/6–31G* (cfm). Characteristic chemical shift of H-C=N- is an important indicator to determine Schiff bases,

because it resonates outside of the aromatic region. In this study, shift of H-C=N- (H9) was observed at 8.38 ppm for experimental ^{1}H NMR spectra of MPA molecule and were calculated as 8.18 (HF/gas), 8.35 (HF/cfm) and 8.00 (B3LYP/gas), 8.10 (B3LYP/cfm) ppm, using the 6–31G* basis set. As seen at the Table 3, there are correlations between the experimental and calculated ^{1}H NMR results and the corresponding R^2 values were found as 0.872 (HF/gas), 0.858 (HF/cfm) and 0.885 (B3LYP/gas), 0.872 (B3LYP/cfm) for the ^{1}H NMR study.

The chemical shift of C atom of bond C=N- is another important indicator to determine Schiff bases. In our study, this shift (C9) was observed at 159.5 ppm for experimental ^{13}C spectra of the MPA molecule, and was calculated as 154.9 (HF/gas), 157.8 (HF/cfm), 148.4 (B3LYP/gas), and 150.2 (B3LYP/cfm) ppm. As seen in the Table 3, there are correlations between the experimental and calculated ^{13}C NMR results and, the corresponding R^2 values were found as 0.980 (HF/gas), 0.981 (HF/cfm), 0.979 (B3LYP/gas) and 0.982 (B3LYP/cfm) for the ^{13}C NMR study. It was understood that calculated ^{13}C NMR results in a solvent (cfm) are slightly better than in gas phase. This is quite normal, because the experimental NMR studies are carried out in a solvent medium.

Table 3. *The experimental and calculated ^{1}H and ^{13}C isotropic chemical shifts (with respect to TMS, all values in ppm) for MPA molecule.*

Atom	Experimental (cfm solvent)	Calculated			
		HF/6-31G*		B3LYP/6-31G*	
		Gas Phase	Solvent (cfm)	Gas Phase	Solvent (cfm)
C1	127.4	128.8	129.7	125.1	125.9
C2	128.9	126.5	127.0	121.9	122.6
C3	129.3	127.2	128.4	122.0	123.3
C4	128.9	126.6	127.0	121.9	122.5
C5	127.4	123.4	124.0	117.8	118.4
C6	135.8	132.7	132.4	129.3	129.2
C7	143.0	139.1	141.4	136.0	137.9
C8	128.8	124.9	123.7	122.5	121.8
C9	159.5	154.9	157.8	148.4	150.2
C10	144.6	139.7	139.8	138.0	137.8
C11	122.2	127.7	127.6	123.5	123.4
C12	114.4	107.3	108.2	103.7	104.6
C13	158.4	152.1	152.4	150.0	150.5
C14	114.4	115.9	116.0	111.8	112.1
C15	122.2	119.3	120.0	111.0	111.7
C16	55.5	48.5	49.0	52.3	50.8
	R^2	*0.980*	*0.981*	*0.979*	*0.982*
H1	7.61	8.16	8.28	7.70	7.80
H2	7.49	7.67	7.79	7.26	7.38
H3	7.46	7.56	7.72	7.20	7.33
H4	7.49	7.59	7.72	7.11	7.26
H5	7.61	7.40	7.59	6.95	7.08
H7	7.20	6.91	7.17	6.52	6.71
H8	8.38	7.22	7.19	6.92	6.90
H9	8.38	8.18	8.35	8.00	8.10
H11	7.29	7.30	7.46	6.93	7.03
H12	7.00	7.12	7.18	6.66	6.73
H14	7.00	6.76	6.97	6.43	6.62
H15	7.29	7.56	7.62	7.09	7.10
H16	3.91	3.61*	3.71*	3.67*	3.76*
	R^2	*0.872*	*0.858*	*0.885*	*0.872*

* Average

4.4. HOMO-LUMO Analysis

The highest occupied molecular orbitals and the lowest-lying unoccupied molecular orbitals are abbreviated as HOMO and LUMO, respectively. They are also named as frontier molecular orbitals (FMO). The FMO have important roles in the electric and optical properties, as well as in quantum chemistry, chemical reactions and UV–VIS spectra [24]. The HOMO containing electrons, represents the ability to donate an electron, whereas, LUMO have not electrons, as an electron acceptor represents the ability to obtain an electron. There is an energy gap between HOMO and LUMO, and this energy gap determines the kinetic stability, chemical reactivity, optical polarizability and chemical hardness–softness of a molecule. It is high for hard molecules and is small for soft molecules [25,26]. A small HOMO-LUMO energy gap automatically means small excitation energies to the manifold of excited states. Therefore, soft molecules have small energy gap, will be more polarizable than hard molecules. High polarizability was the most characteristic property attributed to soft acids and bases [27].

The calculations indicate that the MPA has 63 occupied molecular orbitals. The value of the energy separation between the HOMO and LUMO was found as 9.53 (HF/6-31G*) and 3.52 eV (B3LYP/6-31G*) for MPA. This large energy gap indicates that MPA is quite stable. Lower value in the HOMO and LUMO energy gap explains the eventual charge transfer interactions taking place within the molecule. The LUMO of π nature (i.e. benzene ring) was delocalized over the whole C-C bond, whereas the HOMO was located over methoxy, C=N and its neighbor C=C groups; consequently the HOMO–LUMO translation implies an electron density transfer to C-C bond of the benzene rings from methoxy, C=N and its neighbor C=C groups. The distributions of the HOMO and LUMO were computed both by HF and B3LYP method with 6-31G* basis set for MPA molecule and the results are shown in Fig 4.

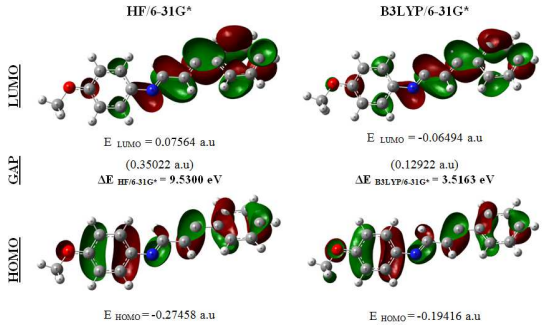

Figure 4. *HOMO-LUMO plot, energy and energy gap of MPA molecule*

In this study, ionization potential (IP), electron affinity (EA), electrophilicity index (ω), chemical potential (μ), electronegativity (χ), chemical hardness (□), and softness (S) were calculated using HOMO and LUMO results of MPA molecule. The IP is calculated as the energy difference between the energy of the molecule derived from

electron-transfer and the respective neutral molecule. The EA is computed as the energy difference between the neutral molecule and the anion molecule. The HOMO and LUMO energies are also used to estimate the IP and EA in the framework of Koopmans'theorem[28]. If IP ≈ $-E_{HOMO}$ and EA ≈ $-E_{LUMO}$ then the average value of the HOMO and LUMO energies is related to the electronegativity (χ) defined by Mulliken[29] with χ = (IP + EA)/2. The HOMO–LUMO gap is related to the hardness (□) [30–33]. The global chemical reactivity parameter has been introduced and was called an electrophilicity index (ω) by Parr et al. [31]. It is define as $\omega = \mu^2/2\eta$ where μ is the chemical potential that is determined as $\mu \approx -\chi = -(IP + EA)/2$. The global softness (S) is the inverse of the global hardness[34] and it can be defined as $S = 1/\eta$. All calculation results are given in Table 4.

Table 4. *The calculated HOMO–LUMO energy and other molecular properties using HF and B3LYP methods with 6-31G* basis set of MPA.*

Parameters	HF	B3LYP
HOMO (eV)	-7.471705114	-5.283364647
LUMO (eV)	2.058269993	-1.767108056
Energy gap (eV)	9.529975107	3.516256591
Electronic energy (a.u.)	-743.903997	-748.678925
Ionization potential, IP (eV)	-7.471705114	-5.283364647
Electron affinity, EA (eV)	2.058269993	-1.767108056
Chemical hardness, η(eV)	-4.764987554	-1.758128296
Chemical potential, μ (eV)	-2.70671756	-3.525236352
Electrophilicity index, ω (eV)	-0.768765906	-3.534239045
Chemical reactivity, S (eV^{-1})	-0.209864137	-0.568786705
Electronegativity, χ (eV)	2.70671756	3.525236352
Dipole moment (Debye)	1.2159	0.7145

5. Conclusion

In this study, structural parameters, vibrational frequencies and ^1H and ^{13}C NMR chemical shift values for 4-methoxy-*N*-(3-phenylallylidene)aniline molecule were calculated, and the HOMO-LUMO analysis of the molecule were also performed by using HF and B3LYP method with 6-31G* basis set. The calculated structural parameters, scaled vibrational frequencies, and chemical shift values have been compared with corresponding experimental values. It is observed that there are no significant differences between the experimental and the theoretical structures. It was noted that some of the experimental results belong to the solid phase, while theoretical calculations were due to gaseous phase. Theoretical ^1H and ^{13}C NMR chemical shift values were carried out and the results were compared with experimental data. Between the experimental and theoretical results was shown to be a good agreement for both ^1H and ^{13}C NMR. The observed and stimulated spectra are in very good agreement for HF and DFT methods. A reasonable agreement was observed between the observed and calculated chemical shifts. Furthermore, the HOMO-LUMO analysis of MPA molecule was performed and the calculated HOMO and LUMO energies was used to semiquantitatively estimate the ionization potential, electron affinity, electronegativity, electrophilicity index, hardness, softness and chemical potential.

Reference

[1] A.S. Munde, A.N. Jagdale, S.M. Jadhav, T.K. Chondhekar, Synthesis, characterization and thermal study of some transition metal complexes of an asymmetrical tetradentate Schiff base ligand, J. Serb. Chem. Soc. 75 (2010) 349–359.

[2] F. Faridbod, M.R. Ganjali, R. Dinarvand, P. Norouzi, S. Riahi, Schiff's Bases and Crown Ethers as Supramolecular Sensing Materials in the Construction of Potentiometric Membrane Sensors, Sensors. 8 (2008) 1645–1703.

[3] R.W. Layer, The Chemistry of Imines., Chem. Rev. 63 (1963) 489–510.

[4] Q. Zhao, C. Shen, H. Zheng, J. Zhang, P. Zhang, Synthesis, characterization, and cytotoxicity of some novel glycosyl thiazol-2-imines as antitumoral agents., Carbohydr. Res. 345 (2010) 437–41.

[5] O. Bekircan, B. Kahveci, M. Küçük, Synthesis and Anticancer Evaluation of Some New Unsymmetrical 3,5-Diaryl-4H-1,2,4-Triazole Derivatives., Turkish J. Chem. 30 (2006) 29–40.

[6] L. Shi, H.-M. Ge, S.-H. Tan, H.-Q. Li, Y.-C. Song, H.-L. Zhu, et al., Synthesis and antimicrobial activities of Schiff bases derived from 5-chloro-salicylaldehyde., Eur. J. Med. Chem. 42 (2007) 558–64.

[7] N. Ghanwate, A. RAUT, A. Doshi, Synthesis and antimicrobial properties of Flavone imines, Orient. J. Chem. 24 (2008) 721–724.

[8] A. Jarrahpour, D. Khalili, E. De Clercq, C. Salmi, J.M. Brunel, Synthesis, antibacterial, antifungal and antiviral activity evaluation of some new bis-Schiff bases of isatin and their derivatives., Molecules. 12 (2007) 1720–30.

[9] G.K. Gomma, M.H. Wahdan, Schiff bases as corrosion inhibitors for aluminium in hydrochloric acid solution., Mater. Chem. Phys. 39 (1995) 209–213.

[10] R.K. Upadhyay, S.P. Mathur, Effect of Schiff's Bases as Corrosion Inhibitors on Mild Steel in Sulphuric Acid, E-J.Chem. 4 (2007) 408–414.

[11] Y. Bekdemir, K. Efil, Microwave Assisted Solvent-free Synthesis of Some Imine Derivatives., Org. Chem. Int. 2014 (2014) 5.

[12] M.J. Frisch, G.W. Trucks, H.B. Schlegel, G.E. Scuseria, M.A. Robb, J.R. Cheeseman, et al., Gaussian 03, Revision E.01, (2004).

[13] R. Dennington II, T. Keith, J. Millam, Gauss View Version 4.1.2, (2007).

[14] J.B. Foresman, Ae. Frisch, Exploring Chemistry With Electronic Structure Methods: A Guide to Using Gaussian, 2nd ed., Gaussian, Inc, Pittsburgh, PA, 1996.

[15] R. Ditchfield, Molecular Orbital Theory of Magnetic Shielding and Magnetic Susceptibility., J. Chem. Phys. 56 (1972) 5688.

[16] K. Wolinski, J.F. Hinton, P. Pulay, Efficient implementation of the gauge-independent atomic orbital method for NMR chemical shift calculations., J. Am. Chem. Soc. 112 (1990) 8251–8260.

[17] Y. Li, X.-L. He, X.-Y. Yang, 4-Methoxy-N-(3-phenylallylidene) aniline., Acta Crystallogr. Sect. E. 63 (2007) o4546.

[18] B.H. Stuart, Infrared Spectroscopy: Fundamentals and Applications (Analytical Techniques in the Sciences (AnTs) *), Wiley & Sons Ltd, Chichester, UK, 2004.

[19] T.N. Sorrell, Organic chemistry, 2nd ed., University Science Books, 2006.

[20] L.H. Abdel-Rahman, R.M. El-Khatib, L.A.E. Nassr, A.M. Abu-Dief, M. Ismael, A.A. Seleem, Metal based pharmacologically active agents: synthesis, structural characterization, molecular modeling, CT-DNA binding studies and in vitro antimicrobial screening of iron(II) bromosalicylidene amino acid chelates., Spectrochim. Acta. A. Mol. Biomol. Spectrosc. 117 (2014) 366–78.

[21] L.D.S. Yadav, Organic Spectroscopy, Springer, 2005.

[22] R.M. Silverstein, F.X. Webster, Spectrometric Identification of Organic Compounds, 6th ed., John Wiley & Sons, Inc, New York, 1998.

[23] R. J Anderson, D. J Bendell, P. W Groundwater, Organic Spectroscopic Analysis., Royal Society of Chemistry, Cambridge, 2004.

[24] I. Fleming, Frontier orbitals and organic chemical reactions, Wiley, London, 1976.

[25] B. Kosar, C. Albayrak, Spectroscopic investigations and quantum chemical computational study of (E)-4-methoxy-2-[(p-tolylimino)methyl]phenol., Spectrochim. Acta A. 78 (2011) 160–167.

[26] N.O. Obi-Egbedi, I.B. Obot, M.I. El-Khaiary, Quantum chemical investigation and statistical analysis of the relationship between corrosion inhibition efficiency and molecular structure of xanthene and its derivatives on mild steel in sulphuric acid., J. Mol. Struct. 1002 (2011) 86–96.

[27] R.G. PEARSON, Absolute electronegativity and hardness correlated with molecular orbital theory., Proc. Nati. Acad. Sci. USA. 83 (1986) 8440–8441.

[28] T. Koopmans, Über die Zuordnung von Wellenfunktionen und Eigenwerten zu den Einzelnen Elektronen Eines Atoms., Physica. 1 (1934) 104–113.

[29] R. Mulliken, A New Electroaffinity Scale; Together with Data on Valence States and on Valence Ionization Potentials and Electron Affinities., J. Chem. Phys. 2 (1934) 782.

[30] R.G. Parr, R.G. Pearson, Absolute hardness: companion parameter to absolute electronegativity, J. Am. Chem. Soc. 105 (1983) 7512–7516.

[31] R.G. Parr, L. v. Szentpály, S. Liu, Electrophilicity Index, J. Am. Chem. Soc. 121 (1999) 1922–1924.

[32] R.G. Parr, W. Yang, Density Functional Theory for Atoms and Molecules, Oxford University Press, New York, 1982.

[33] R.G. Pearson, Chemical hardness, John Wiley-VCH, Weinheim, 1997.

[34] A. Lesar, I. Milošev, Density functional study of the corrosion inhibition properties of 1,2,4-triazole and its amino derivatives, Chem. Phys. Lett. 483 (2009) 198–203.